Available online at www.sciencedirect.com

SCIENCE DIRECT®

Materials Letters 58 (2004) 3074–3078

materials letters

www.elsevier.com/locate/matlet

Optical damage resistance of In:Fe:$LiNbO_3$ crystals related to the defect structure

T. Zhang[a], B. Wang[a,*], S.Q. Fang[a], D.C. Ma[a], Y.Q. Zhao[a], Y.H. Xu[a,b]

[a] *Electro-Optics Technology Center, Harbin Institute of Technology, Harbin 150001, PR China*
[b] *Applied Chemistry Department, Harbin Institute of Technology, Harbin 150001, PR China*

Received 13 November 2003; received in revised form 4 May 2004; accepted 9 May 2004

Abstract

A series of In:Fe:$LiNbO_3$ crystals with various concentration of In_2O_3 doping were grown in an air atmosphere using the Czochralski method. Spectroscopic properties (fundamental absorption edge, OH vibrational band) were used for an exploration of the defect structure. Light-induced scattering and direct observation of the transmitted laser beam distortion were used to characterize the optical damage. It was found that the threshold intensity of In (3 mol%):Fe:$LiNbO_3$ was 2 orders of magnitude higher than that of Fe:$LiNbO_3$ and was able to withstand higher power level. The increase in damage resistance could be attributed to the Fe^{3+} losing their electron acceptor properties and therefore an increase in photoconductivity.

PACS: 42.70.Nq; 42.25.Fx; 74.62.Dh
Keywords: In:Fe:$LiNbO_3$; Optical damage; Defect structure

---

1. Introduction

The combination of excellent linear, nonlinear properties, and good mass productivity of lithium niobate ($LiNbO_3$) single crystals has made them important for extensive industrial applications [1–4]. However, when $LiNbO_3$ devices, such as frequency doubling converters, waveguide lasers, optical switches, and parametric oscillators, are operated at a high laser intensity, their optical performance is severely restricted by the laser-induced refractive index inhomogeneity, which has been labeled “optical damage” or “photorefraction.” Investigations of these photorefractive effects have pointed out the involvement of a variety of impurities and intrinsic defects [5], and past efforts to reduce or even eliminate the problem have mainly focused on both purification of the starting materials for the crystal growth and post-growth treatments, such as oxidation or electro-diffusion [6,7]. Since it has been reported that $LiNbO_3$ doped with 4.6 mol% MgO has the ability to resist light intensity about 100 times greater than pure $LiNbO_3$ [8], doping impurity ions into crystals to affect photorefractive properties receives a lot of interest. Other optical damage resistance impurities, Zn [9] and Sc [10], have been found subsequently. Indium reported by Volk and Rubinina [11] is a new kind of impurity similar to Mg and Zn and can noticeably reduce the photorefractive effect in $LiNbO_3$ crystals. These authors demonstrated that Zn (6.5 mol%):Fe (0.01 wt.%):$LiNbO_3$ co-doped with 1.5 mol% In could reduce optical damage comparable to that of Zn (7.2 mol%):Fe (0.01 wt.):$LiNbO_3$.

In general, the photorefractive effect in $LiNbO_3$ crystals is due to the space charge formed between the acceptor centers that trap free electrons and the donor centers that release electrons, which are excited by the laser beam irradiation [12]. Doping ions incorporated into the host lattice of $LiNbO_3$ will result in a large amount of extrinsic defects, change the environment around photorefractive center ions, and therefore affect the photorefractive effect. Thus, it will be of great interest to investigate the correlation between the changes in defect structure of crystals and photorefraction.

In this paper, the infrared transmittance spectra and ultraviolet–visible absorption spectra were measured in order to investigate the defect structure of the crystals. The effect of doping In ions on the optical damage resistance of In:Fe:$LiNbO_3$ crystals was systematically discussed.

---

* Corresponding author.
E-mail address: tzhang_hit02@yahoo.com (B. Wang).

0167-577X/$ - see front matter © 2004 Elsevier B.V. All rights reserved.
doi:10.1016/j.matlet.2004.05.046

2. Experimental details

2.1. Crystal growth and sample preparation

In:Fe:$LiNbO_3$ crystals were grown in an automatic diameter control (ADC) system using the conventional Czochralski method in an air atmosphere. The starting materials used were all ultrapure. The congruent ratio of Li/Nb = 0.946 (molar ratio) was selected as melt composition. Fixed 0.03 wt.% Fe_2O_3 and varying levels of In_2O_3 (0.5, 1, and 1.5 mol%) were added to the melt, respectively. After being weighed accurately and mixed thoroughly for 12 h, the materials were put into a platinum crucible (60 mm in diameter and 40 mm in height) and calcined at 700 °C for 2 h to decompose the carbonate; they were then sintered at 1150 °C for 2 h to form polycrystalline bulk.

The crystal was pulled along [001] direction at a rate of ~ 2 mm/h, rotated at a rate of ~ 20 rpm, and the temperature gradient above melt surface was about 35–40 °C/cm. After growth, the crystals were cooled down to room temperature at a rate of 80 °C/h; they were then polarized in another resistive furnace in which the temperature gradient was almost close to zero using an applied DC electric current density of 5 mA/cm^2 for 30 min at 1200 °C. All as-grown crystals appeared to be transparent, crack-free, and inclusion-free. Lastly, from the middle of the crystals, they were y-cut into slices with the size of $10 \times 2 \times 10$ mm^3 ($a \times b \times c$). The (010) faces were ground using SiC powder and then polished to optical grade using a 0.25-μm diamond solution for experimental characterization. Table 1 listed the growth conditions for these crystals.

2.2. Measurement

The infrared transmittance spectra of the crystals were recorded by a Fourier infrared spectrometer with a wave number range of 3000–4000 cm^{-1} at room temperature. The nonpolarized light ultraviolet–visible absorption spectra of In:Fe:$LiNbO_3$ crystals were measured with a wavelength range of 350–500 nm by a CARYIE-model UV–Visible spectrophotometer at room temperature.

The optical damage resistance of the crystals was characterized by measuring the light-induced scattering intensity change as a function of the incident light intensity. A schematic drawing of the experimental arrangement is shown in Fig. 1. An argon-ion laser at the wavelength of 514.5 nm was used as light source, and the incident beam power level could be adjusted by an attenuator. The crystal *c*-axis was set parallel to the polarization direction of the laser beam and placed on the back focal plane of the convex lens. The power density of the beam spot passing through a pinhole on a light shield was measured by a photodiode connected with a computer. When the laser intensity reached or exceeded a certain value, the transmitted beam spot through the crystal was smeared and elongated along the *c*-axis, with a decrease in the intensity at the central part: the optical damage phenomenon thus occurred inside the crystal.

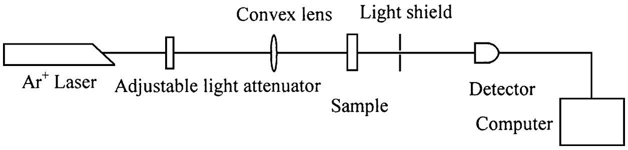

Fig. 1. Experimental setup.

Table 1
Crystal growth conditions for In:Fe:$LiNbO_3$ crystals

Sample	No. 1	No. 2	No. 3	No. 4
[Fe_2O_3] in melt (wt.%)	0.03	0.03	0.03	0.03
[In_2O_3] in melt (mol%)	0	0.5	1.0	1.5
Melt weight (g)	530	540	530	550
Heating equipment	RF[a]	RF	RF	RF
Crystal size (mm^2)	Ø30 × 30	Ø30 × 35	Ø30 × 30	Ø30 × 32
Growth atmosphere	Air	Air	Air	Air
Seeding temperature (°C)	1240	1250	1254	1246

[a] RF denotes resistive furnace using SiC rods.

3. Results and discussion

3.1. Infrared transmittance spectra

The infrared transmittance spectra of crystals mainly reflect the vibrational absorption peak change of OH combined with the defect group and can suggest the doping ions location in the crystal lattice [13]. Fig. 2 shows the infrared transmission spectra of these crystals. Nos. 1–3 crystals revealed similar positions of the OH absorption peak at approximately 3482 cm^{-1}, while in the case of the No. 4 crystal, the absorption peak position was somewhat different, which shifted to 3507 cm^{-1}.

Many intrinsic defects, such as anti-site Nb and Li vacancies, existed in the $LiNbO_3$ crystals. The H^+ ions congregated around Li vacancies due to their electronegativity and formed $(V_{Li})^-$–OH^- complexes, which corresponded to the vibrational absorption peak at 3482 cm^{-1}

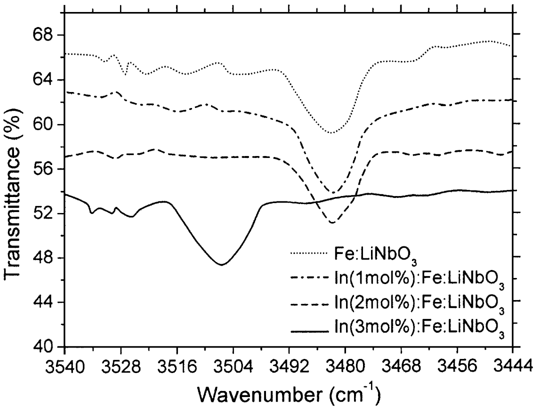

Fig. 2. Infrared transmittance spectra of crystals.

[14]. When In ions entered the crystal lattices, below the threshold concentration (Nos. 2 and 3), they substituted anti-site Nb and existed in form of $(In_{Li})^{2+}$. The H^+ ions did not assemble around these defects because of being repelled by them. So the IR absorption peak still reflected the vibration of the above-referred complexes at the same position. When the concentration of In^{3+} ions exceeded the threshold (No. 4), after the anti-site Nb's were canceled, a part of In^{3+} ions occupying Nb sites formed $(In_{Nb})^{2-}$ defects. Because the defects had a stronger force to attract H^+ than $(V_{Li})^-$, the H^+ ions drifted to the $(In_{Nb})^{2-}$ defects, and the $(In_{Nb})^{2-}$–OH^- complexes were formed, which was mainly responsible for OH^- absorption peak of 3507 cm^{-1}.

3.2. Ultraviolet–visible absorption spectra

Fig. 3 shows the nonpolarized light ultraviolet–visible absorption spectra of the crystals. It can be clearly seen that the absorption edges of Nos. 2–4 crystals successively shifted to the violet band, in comparison with that of the No. 1 crystal.

As is well known, the absorption edge in $LiNbO_3$ corresponds to the electron transition from the valence band (p state of the oxygen ion) to the conduction band (d state of the transition-metal niobate ions) under the action of photons, and the intensity of the Nb–O bond will affect the energy gap between the valence band and the conduction band, i.e. the forbidden band gap [15]. Therefore, the valence electronic state of oxygen ions will directly influence the position of the absorption edge. In Fe:CLN, when Fe ions were incorporated into the lattice of crystal, two valences of Fe (Fe^{2+} and Fe^{3+}) substituted Li ions and located Li sites [16]. This increased the deformation level of the electron clouds of oxygen ions and resulted in a decrease in the energy gap since the polarization ability of Fe ions was greater than that of the Li ions. The absorption edge thus shifted to the red band, compared with the undoped $LiNbO_3$. In the case of In:Fe:$LiNbO_3$ crystals, instead, In ions below the threshold concentration preferentially replaced anti-site Nb ions and occupied Nb_{Li} sites. As the In-doped concentration was increased, Fe ions on the Li sites would be repelled by the In ions to the Nb sites. When the concentration of In doping was over the threshold, after the removal of Nb_{Li}, the additional In ions and most of the Fe ions occupied Nb sites. This decreased the deformation level of the electron clouds of the oxygen ions and the energy gap due to the polarization ability of the In ions less than that of the Nb ions. Thus, the absorption edges of Nos. 2–4 shifted gradually towards the violet band.

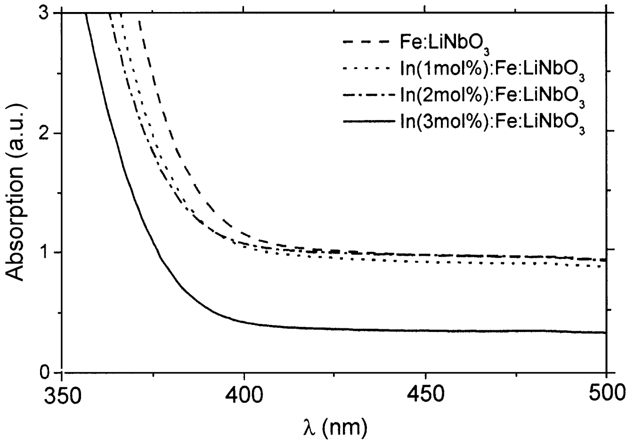

Fig. 3. Ultraviolet–visible absorption spectra of crystals.

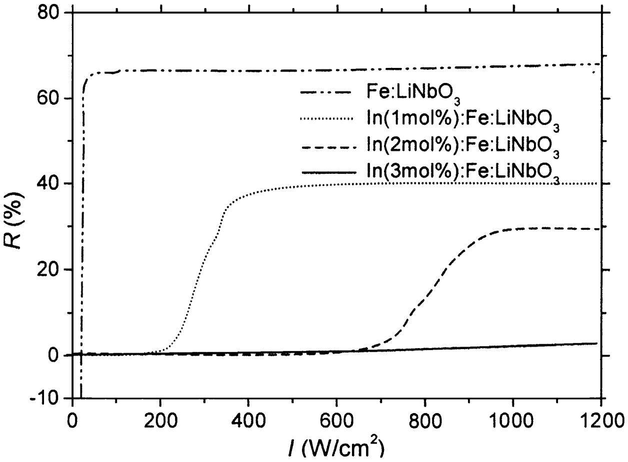

Fig. 4. Dependence of the ratio R of the light-scattered intensity to the incident light intensity vs. the incident light intensity.

3.3. Optical damage resistance of crystals

When $LiNbO_3$ crystals are used as holographic storage media, higher light-induced scattering resistance ability can improve the quality of the storage information, suppress the generation of noise, and reduce the bit error rate. To estimate the ability of these crystals to resist photorefraction, the light-induced scattering change of a transmitted laser beam through the 2-mm-thick plates of these crystals was measured (see Fig. 1). Fig. 4 gives the ratio R of the light-scattered intensity I' to the incident light intensity I, $R = I'/I$, in the crystals as a function of I.

From Fig. 4, it can be observed that the threshold intensity, which induced the transmitted beam scattering, increases with an increase in the In doping level in the crystals. When the In doping concentration was up to 3 mol%, the threshold intensities of In (3 mol%):Fe:$LiNbO_3$ (No. 4) were 2 orders of magnitude higher than that of Fe:$LiNbO_3$ (No. 1). Furthermore, even if the incident light intensity exceeded the above-mentioned threshold intensity, the light-scattered intensity in highly doped $LiNbO_3$ crystal was also much weaker than that of Fe-doped $LiNbO_3$ (see Fig. 4).

The distortion of the Ar^+ ion laser beam at the same power level for the equal time of irradiation on these crystals was shown in Fig. 5. Fe:$LiNbO_3$ (No. 1) displayed a severe diffusion along the *c*-axis [Fig. 5(a)]. For In:Fe:$LiNbO_3$

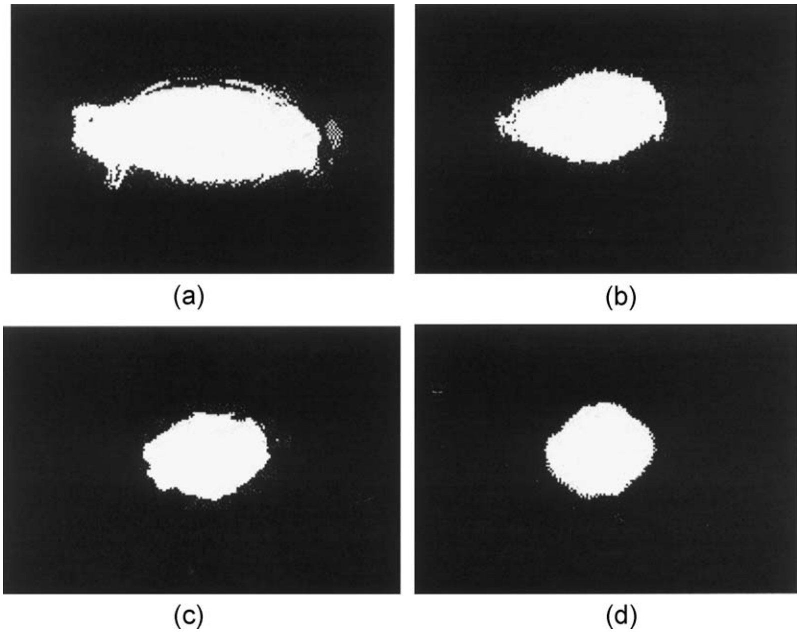

Fig. 5. Distortion of the transmitted Ar^+ ion laser beam spots. (a) Fe:$LiNbO_3$ (No. 1); (b) In (1 mol%):Fe:$LiNbO_3$ (No. 2); (c) In (2 mol%):Fe:$LiNbO_3$ (No. 3); (d) In (3 mol%):Fe:$LiNbO_3$ (No. 4).

crystals, lower In doping concentration's crystals (Nos. 2 and 3) showed slight distortion in the beam [Fig. 5(b) and (c)], while In (3 mol%):Fe:$LiNbO_3$ (No. 4) was found to be able to withstand the same laser power level without obvious beam smearing [Fig. 5(d)].

In Fe-doped $LiNbO_3$, Fe^{3+} ions are the most probable electron acceptors. Other doping ions incorporated into the host lattice will change the substitution site of electron acceptor Fe^{3+}. An abrupt decrease in the capture cross section of electrons by Fe^{3+} is then responsible for the observed increase in photoconductivity and therefore causes the increase in resistance ability to optical damage [17]. From the above discussion in Sections 3.1 and 3.2, it could be seen that below the In^{3+} threshold concentration, a portion of Fe^{3+} ions still occupied Li sites; the Fe^{3+} ions did not completely lose their electron acceptor properties, and therefore the resistance ability to the optical damage of Nos. 2 and 3 crystals did not noticeably improve despite the increase in photoconductivity [see Figs. 4, 5(b) and (c)]. As the In doping level increased to 3 mol%, most of Fe^{3+} ions were all pushed to Nb sites and lost their electron acceptor properties since $(Fe_{Nb})^{2-}$ defects were electronegative. This drastically increased the photoconductivity. Therefore, the resistance ability to optical damage of the No. 4 crystal was much higher than that of the Nos. 2 and 3 crystals [see Figs. 4 and 5(d)].

4. Conclusions

In conclusion, we grew crack-free and inclusion-free In, Fe co-doped $LiNbO_3$ single crystals and studied the behavior of OH vibrational band, fundamental absorption edge, and optical damage as a function of In_2O_3 doping concentration. It was assumed that In^{3+} ions initially occupied Nb_{Li} sites and then replaced Nb sites when In doping was up to the threshold concentration (3 mol%). Simultaneously, most of Fe^{3+} ions were repelled to Nb sites from Li sites and lost their electron acceptor properties. This caused an increase in the photoconductivity. Therefore, the threshold intensity of In (3 mol%):Fe:$LiNbO_3$ was 2 orders of magnitude higher than that of Fe:$LiNbO_3$.

Acknowledgements

This study was sponsored by the National Research for Fundamental Key Projects No. 973 (G19990330), the National Advanced Technology Program No. 863 (2001AA31304), the National Natural Science Foundation (10172030, 50232030), and the Nature Science Foundation of Heilongjiang Province (A01-01), P.R. China.

References

[1] M.H. Li, Y.H. Xu, R. Wang, X.H. Zhen, C.Z. Zhao, Cyst. Res. Technol. 36 (2001) 191.
[2] M.N. Armenise, C. Canali, M. De Sario, E. Zanoni, Mater. Chem. Phys. 9 (1983) 267.
[3] T.Y. Fan, A. Cordova-Plaza, M.J.F. Digonnet, R.L. Byer, H.J. Shaw, J. Opt. Soc. Am. B 3 (1986) 140.
[4] L.E. Myers, G.D. Miller, R.C. Echardt, M.M. Fejer, R.L. Byer, W.R. Bosenberg, Opt. Lett. 20 (1995) 52.
[5] G.E. Peterson, A.M. Glass, A. Carnevale, P.M. Bridenbaugh, J. Am. Ceram. Soc. 56 (1973) 278.

[6] P.J. Jorgensen, R.W. Bartlett, J. Phys. Chem. Solids 30 (1969) 2639.

[7] R.G. Smith, D.B. Fraser, R.T. Denton, T.C. Rich, J. Appl. Phys. 39 (1968) 4600.

[8] G.G. Zhong, J. Jian, Z.K. Wu, 11th International Quantum Electronics Conference, New York, 1980, IEEE Cat. No. 80, CH 1561-0, P631.

[9] T.R. Volk, N.M. Rubinina, V.L. Pryalkin, V.V. Krasnikov, V.V. Volkov, Ferroelectrics 109 (1990) 345.

[10] J.K. Yamamoto, K. Kitamura, N. Iyi, S. Kimura, Y. Furukawa, M. Sato, Appl. Phys. Lett. 61 (1992) 2156.

[11] R. Volk, N.M. Rubinina, Ferroelectr. Lett. 14 (1992) 37.

[12] Y. Ohmori, M. Yamaguchi, K. Yoshino, Y. Inuishi, Jpn. J. Appl. Phys. 18 (1979) 79.

[13] L. Kovács, L. Rebout, J.C. Soares, M.F. da Silva, M. Hage-Ali, J.P. Stoquert, P. Siffert, J.A. Sanz-Garcia, G. Corradi, Zs. Szaller, K. Polgár, J. Phys.: Condens. Matter 5 (1993) 781.

[14] O.F. Schirmer, O. Thiemann, M. Wohlecke, J. Phys. Chem. Solids 52 (1991) 185.

[15] M. Didomenico, S.H. Wemple, J. Appl. Phys. 40 (1969) 720.

[16] C. Prieto, C. Zaldo, Solid State Commun. 83 (1992) 819.

[17] T. Volk, N. Rubinina, M. Wöhlecke, J. Opt. Soc. Am. B 11 (1994) 1681.